INTERMEDIATE MASS DIMUONS IN NA38/NA50

C.Soave[11] - NA50 collaboration

M.C. Abreu[6,a], B. Alessandro[11], C. Alexa[3], R. Arnaldi[11], J. Astruc[8], M. Atayan[13], C. Baglin[1], A. Baldit[2], M. Bedjidian[12], F. Bellaiche[12], S. Beolè[11], V. Boldea[3], P. Bordalo[6,b], A. Bussière[1], V. Capony[1], L. Casagrande[6], J. Castor[2], T. Chambon[2], B. Chaurand[9], I. Chevrot[2], B. Cheynis[12], E. Chiavassa[11], C. Cicalò[4], M.P. Comets[8], S. Constantinescu[3], J. Cruz[6], A. De Falco[4], N. De Marco[11], G. Dellacasa[11,c], A. Devaux[2], S. Dita[3], O. Drapier[12], B. Espagnon[2], J. Fargeix[2], S.N. Filippov[7], F. Fleuret[9], P. Force[2], M. Gallio[11], Y.K. Gavrilov[7], C. Gerschel[8], P. Giubellino[11], M.B. Golubeva[7], M. Gonin[9], A.A. Grigorian[13], J.Y. Grossiord[12], F.F. Guber[7], A. Guichard[12], H. Gulkanyan[13], R. Hakobyan[13], R. Haroutunian[12], M. Idzik[11,d], D. Jouan[8], T.L. Karavitcheva[7], L. Kluberg[9], A.B. Kurepin[7], Y. Le Bornec[8], C. Lourenço[5], M. Mac Cormick[8], P. Macciotta[4], A. Marzari-Chiesa[11], M. Masera[11], A. Masoni[4] , S. Mehrabyan[13], S. Mourgues[2], A. Musso[11], F. Ohlsson-Malek[12,e], P. Petiau[9], A. Piccotti[11], J.R. Pizzi[12], W.L. Prado da Silva[11,f], G. Puddu[4], C. Quintans[6], C. Racca[10], L. Ramello[11,c], S. Ramos[6,b], P. Rato-Mendes[11], L. Riccati[11], A. Romana[9], S. Sartori[11], P. Saturnini[2], E. Scomparin[5,g], S. Serci[4], R. Shahoyan[6,h], S. Silva[6], C. Soave[11], P. Sonderegger[5,b], X. Tarrago[8], P. Temnikov[4], N.S. Topilskaya[7], G.L. Usai[4], C. Vale[6], E. Vercellin[11], N. Willis[8].

[1] *LAPP, CNRS-IN2P3, Annecy-le-Vieux, France.*
[2] *LPC, Univ. Blaise Pascal and CNRS-IN2P3, Aubière, France.*
[3] *IFA, Bucharest, Romania.*
[4] *Università di Cagliari/INFN, Cagliari, Italy.*
[5] *CERN, Geneva, Switzerland.*
[6] *LIP, Lisbon, Portugal.*
[7] *INR, Moscow, Russia.*
[8] *IPN, Univ. de Paris-Sud and CNRS-IN2P3, Orsay, France.*
[9] *LPNHE, Ecole Polytechnique and CNRS-IN2P3, Palaiseau, France.*
[10] *IReS, Univ. Louis Pasteur and CNRS-IN2P3, Strasbourg, France.*
[11] *Università di Torino/INFN, Torino, Italy.*
[12] *IPN, Univ. Claude Bernard and CNRS-IN2P3, Villeurbanne, France.*
[13] *YerPhI, Yerevan, Armenia.*
a) also at FCUL, Universidade de Lisboa, Lisbon, Portugal
b) also at IST, Universidade Técnica de Lisboa, Lisbon, Portugal
c) Dipartimento di Scienze e Tecnologie Avanzate, II Facoltà di Scienze, Alessandria, Italy
d) now at Faculty of Physics and Nuclear Techniques, University of Mining and Metallurgy, Cracow, Poland
e) now at ISN, Univ. Joseph Fourier and CNRS-IN2P3, Grenoble, France
f) now at UERJ, Rio de Janeiro, Brazil
g) on leave of absence from Università di Torino/INFN, Torino, Italy
h) on leave of absence of YerPhI, Yerevan, Armenia

The NA38/NA50 experiments have measured the dimuon production in ultrarelativistic proton–nucleus and nucleus–nucleus collisions at the CERN SPS for different systems and energies. We present here the analysis of the intermediate mass region ($1.5 < M < 2.5\ GeV/c^2$) for the 450 GeV/c p - $A(A = Al, Cu, Ag, W)$, 200 $A\ GeV/c$ S - U and 158 $A\ GeV/c$ Pb - Pb data sets. We show that, after background subtraction, the intermediate mass region can be simply described as a superposition of dimuons from the semi–leptonic decays of charmed meson pairs and DY. No other contribution, as thermal dimuons, has been taken into account. We find that the open charm yield in nucleus–nucleus collisions exceeds a linear extrapolation from proton–nucleus, while in proton–nucleus collisions it is consistent with previous FNAL and CERN experimental results. The intermediate mass region enhancement increases with the system size and c.m. energy up to a factor of $\simeq 3$ in central Pb - Pb collisions. For events in the same mass range, a comparison of the Pb - Pb PYTHIA generated and experimental p_T differential distributions is also shown.

1 Introduction

The NA50 experiment at the CERN SPS studies the muon pair production in nucleus–nucleus collisions to probe the behaviour of nuclear matter under extreme conditions of energy density. Dimuons generated in the interaction volume interact weakly with the hot surrounding medium; they can thus escape undisturbed, carrying out informations about the state of the matter where they were generated [1]. The dimuon mass spectrum can be roughly subdivided in three main regions :

the Low Mass Region (LMR) below the ϕ resonance, the Intermediate Mass Region (IMR) between the ϕ and the J/ψ and the High Mass Region (HMR) above the J/ψ. While the latter can be seen as a simple superposition of high mass DY, J/ψ and ψ', the former originate from different sources (hadron Dalitz decays, charmed meson semi–leptonic decays and DY) with individual shapes and relative contributions not immediatly deductable from the data.

In this paper we study the IMR for the 450 GeV/c p - $A(A = Al, Cu, Ag, W)$, 200 A GeV/c S - U and 158 A GeV/c Pb - Pb data sets. We assume the intermediate mass region to be a superposition of dimuons from DY, charmed hadron decays and combinatorial background. Thermal dimuons, which are expected to appear in nucleus–nucleus collisions, have not been taken into account. Monte–Carlo techniques have been used to generate the DY and open charm mass shapes. The Monte–Carlo generated shapes have then been used to fit the data in order to determine their relative contributions. The opposite–sign background shape has been deduced from the like–sign experimental distributions. The background relative contribution has been fixed with a Monte–Carlo simulation. A similar procedure has been used by the HELIOS-3 collaboration [2]. In the previous NA38/NA50 IMR analysis [3,4] the combinatorial background contribution was estimated without using the Monte–Carlo techniques detailed in paragraph 4.

2 The experimental set–up

The NA38/NA50 experimental apparatus is based on the NA10 muon spectrometer [5]. It consists of a toroidal deflecting magnet, 8 $MWPC$'s and 4 trigger hodoscopes. It is separated from the target region by a 4 m long hadron absorber made of Carbon followed by 0.8 m of Iron. A segmented active target allows the primary vertex identification thanks to a system of quartz blades located after each subtarget. A beam hodoscope (BH) tags incident ions and rejects the beam pile-up. An electromagnetic calorimeter, EMC, measures the neutral transverse energy. In NA38 this was the only way of estimating the collision centrality. In NA50 two more detectors have been included, a multiplicity detector, MD [6], and a zero degree calorimeter, ZDC [7].

In the following the most important differences between the NA38 and NA50 set–ups are listed. For a more detailed description see ref.8,9.

2.1 S - U 200 A GeV/c (NA38)

In the S - U set–up, the segmented active target was made of 12 U subtargets with a total thickness of 0.2 λ_i. The centrality of the collision was measured by an electromagnetic calorimeter located in front of the hadron absorber and covering the pseudorapidity interval $1.7 < \eta < 4.1$. The beam hodoscope and the target detectors were made of plastic scintillator. Muon pairs were detected in the pseudorapidity interval $2.8 < \eta < 4.0$. The field in the toroidal magnet was 1.2 Tm. The beam intensity was about 10^8 $S\ ions/burst$, with a 5 s spill.

2.2 p - A 450 GeV/c and Pb - Pb 158 A GeV/c (NA50)

In the Pb - Pb set–up, the segmented active target is made of 7 Pb subtarget with a total thickness of 0.3 λ_i [10]. The pseudorapidity coverage of the EMC has been shifted to $1.1 < \eta < 2.3$. The beam hodoscope and the active target detectors have been re–built using quartz in order to stand the high radiation level. The field in the toroidal magnet is 2.1 Tm to improve the mass resolution and reduce the rate of soft background muons. A zero degree calorimeter is located along the beam axis in the hadron absorber internal core. It measures the energy of the projectile spectators of the collision and thus estimates the collision centrality. The beam intensity is $5 \cdot 10^7$ $Pb\ ions/burst$, with a 5 s spill.

A similar set–up has been adopted for the p - A data taking. The beam intensity is about $3{\cdot}10^9$ $protons/burst$, with a 2.5 s spill. The active target is replaced by a single target, with no vertex identification system. Four nuclear targets have been used, namely Al, Cu, Ag and W, with thicknesses ranging from 32 g/cm^2 (Al) to 80 g/cm^2 (W).

3 Data reduction and centrality selection

For both proton–nucleus and nucleus–nucleus samples, the selected events must have two and only two fully reconstructed tracks in the muon spectrometer; furthermore, the two tracks must point to the target. These quality cuts are very effective since they reject more than 50% of the triggered events. For nucleus-nucleus collisions, the BH rejects the beam pile-up. In S - U data reduction, the information given by the target detectors has been used to select events with an interaction in one of the subtargets. This method has a low efficiency for peripheral collisions. For this reason, in Pb - Pb data reduction a less restrictive selection has been applied: since events originating from the target region must be strongly correlated in the E_T vs. E_{ZDC} plane, only the events lying in a 2σ region around the average correlation are retained. In order to reject dimuons from kinematical regions where the acceptance is very low, only events with $-0.5 < cos\theta_{CS} < 0.5$ have been accepted, where θ_{CS} is the polar angle of the muons relative to the beam axis in the rest frame of the dimuon. For the same reason, the rapidity cuts $0 < y_{cm} < 1$ for S - U and Pb - Pb

and $-0.52 < y_{cm} < 0.48$ for p - A collisions have been applied.

The S - U and Pb - Pb data sets have been subdivided in 5 and 9 centrality classes respectively corresponding to different E_T bins. The average number of participants and impact parameter for each centrality class have been estimated by means of a geometrical model [11], taking into account realistic nuclear densities. The results have been further checked using a simulation based on the VENUS 4.02 [12] event generator.

4 Combinatorial background

One of the most important contributions to the IMR opposite–sign dimuon spectrum is the background from pion and kaon decays. In p - A collisions at 450 GeV/c, its contribution to the IMR amounts to 85% and to 90% in the most central Pb - Pb collisions at 158 A GeV/c. The background subtraction from the opposite–sign dimuon mass spectrum is usually made using the like–sign dimuon mass distributions. This is due to the fact that π and K decays contribute both to the opposite and to the like–sign dimuon spectra. While the opposite–sign distribution is the superposition of many different sources, like–sign muon pairs are purely due to combinatorial background.

For p - A and S - U data the following formula has been used to estimate the opposite–sign background from the like–sign dimuon distributions,

$$N^{+-} = 2\sqrt{N^{++}N^{--}} \tag{1}$$

In Pb - Pb, where a better degree of accuracy is needed because of the higher background contribution, the opposite–sign distributions have been obtained with mixed event techniques [13]. Eq.1 has then been used for normalization. In fact, eq.1 is strictly valid if there are no acceptance biases introduced by the apparatus and if the $K's$ and $\pi's$ produced in the collision are not charge correlated. While the first condition is satisfied in NA38/NA50 thanks to a suited off-line cut, the second one can be unsatisfied in p - A and peripheral A - B collisions where the produced particle multiplicity is not high enough. For this reason, eq.1 has to be multiplied by a factor $R \geq 1$. A detailed Monte–Carlo simulation has been carried out to compute the background R factor in each particular case. For each of the analysed systems $\simeq 10^5$ VENUS events have been generated and the produced $K's$ and $\pi's$ stored. Each K and π has been tracked through the apparatus and the corresponding decay probabilities into muons, P_{μ_i} with $i = 1, N_\pi + N_K$, have been computed. Within each event, $K's$ and $\pi's$ have been exhaustively combined in opposite and like–sign pairs and subsequently forced to decay. Each dimuon has been given a relative weight equal to the product of its parents decay probabilities $P_{\mu\mu_{i,j}} = P_{\mu_i}P_{\mu_j}$. The dimuon kinematical variables have been computed and the same kinematical cuts as imposed on the experimental data have been applied. With the opposite–sign and like–sign surviving dimuons, the Monte–Carlo background R factor has been evaluated as

$$R^{MC} = \frac{\sum_{n=1}^{N}\sum_{i,j}P^{+-}_{\mu\mu_{i,j}}}{2\sqrt{(\sum_{n=1}^{N}\sum_{i,j}P^{++}_{\mu\mu_{i,j}})(\sum_{n=1}^{N}\sum_{i,j}P^{--}_{\mu\mu_{i,j}})}} \tag{2}$$

where N is the number of generated VENUS events.

For A - B systems, where R is expected to depend on the collision centrality, several calculations have been worked out for different values of the impact parameter b. The R $vs.$ b correlation for S - U and Pb - Pb have been derived. For each centrality class, the average value $\langle R^{MC}\rangle$ has been computed as a weighted average of $R^{MC}(b)$ over the b distribution of the events in that class. As expected, $\langle R^{MC}\rangle$ turns out to be compatible with 1 for central Pb - Pb collisions and larger than 1 for peripheral ones ($\langle R^{MC}\rangle$=1.035 for $\langle b\rangle = 10.7$ corresponding to the most peripheral bin).

The NA50 p - A data have been collected with a high beam intensity and no pile-up rejection. Particles produced in consecutive events can thus pile-up and be seen as originating from a single event. This smears the $K's$ and $\pi's$ charge correlation and reduces the R factor value. Introducing this effect in our simulation, we obtain $\langle R^{MC}\rangle = 1.05$ for p–W collisions at the experimental beam intensity while $\langle R^{MC}\rangle = 1.21$ when pile-up effects are not taken into account.

5 Data analysis

5.1 Introduction

We describe the IMR as a simple superposition of dimuons from charmed meson (and baryon) pair decays and DY, after background subtraction. In order to exclude the contribution of the low mass resonances, the fit starting point has been fixed at 1.5 GeV/c^2. The DY and open charm mass shapes are taken from PYTHIA event generator. The J/ψ and ψ' mass shapes have also been generated, using the method explained in ref.11. The fit of the mass spectra extends up to 8 GeV/c^2 and allows the determination of the DY and open charm contributions as free parameters. The pure DY high mass region ($4.5 < M < 8.0$ GeV/c^2) constrains the DY normalisation. It has been shown [14] that the high mass DY, after isospin correction, scales with A in p - A and with $A \times B$ in A–B collisions. The open charm cross-section

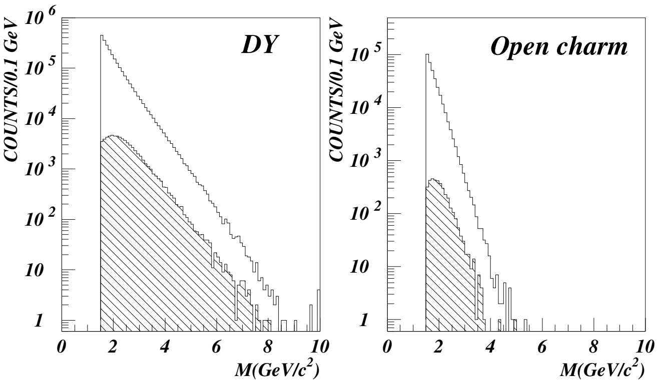

Figure 1: *Generated (plain histogram) and reconstructed (filled histogram) DY and open charm dimuon invariant mass spectra for the Pb - Pb set–up.*

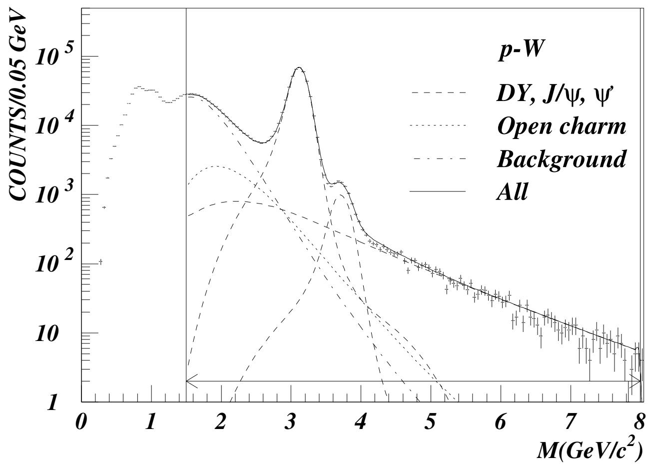

Figure 2: *Fit to the p–W invariant mass spectrum, with the background contribution fixed using R^{MC}. The double arrow indicates the fitted mass range.*

also scales with A in p - A interactions [15] and is expected to scale as $A \times B$ in A–B collisions.

5.2 DY and open charm mass shapes

The DY and open charm mass shapes have been obtained using PYTHIA [16] with the MRS A set of PDFs [17], with m_c=1.5 GeV/c^2 and $\langle k_T^2 \rangle$=0.8 GeV^2. For each process, a large sample of PYTHIA events has been generated. The generation extends over a kinematical window wider than the experimental one in order to account for multiple scattering smearing effects. The generated dimuons have been tracked and reconstructed through the apparatus following the same procedure used for experimental data. In fig.1 the DY and open charm generated and reconstructed mass spectra are shown for the Pb - Pb set–up and for $M > 1.5$ GeV/c^2. The acceptance for a single process is defined as the ratio of reconstructed to generated events in the experimentally covered phase space. For the Pb - Pb set–up and for $M > 1.5$ GeV/c^2, the resulting DY and open charm acceptances are $A_{DY} = 0.028$ and $A_{D\overline{D}} = 0.011$. For p - A a similar result has been obtained as the Pb - Pb and p - A set–ups are practically identical. The S - U set–up has acceptances $\simeq 4$ times higher due to the significantly lower magnetic field.

5.3 Fit of the mass spectra

The four analysed 450 GeV/c p - $A(A = Al, Cu, Ag, W)$ sets of data have been taken with the same experimental set–up. Moreover, as previously said, it has been shown that the DY [18,14] and open charm cross sections [15] scale with A in p - A collisions. The four data sets are therefore fitted simultaneously with the constraint that the ratio $\sigma_{D\overline{D}}/\sigma_{DY}$, left as a free parameter in the fit, is the same in the four samples of events. The J/ψ, ψ' and DY normalizations and the J/ψ mass and width are also left free. The combinatorial background R factors have been either imposed using the results of the simulation, or left as additional free parameters. In both cases a satisfactory description of the mass spectra has been achieved even if, as expected, a better χ^2 is obtained when leaving R free. The normalization of the open charm contribution varies by $\sim$ 20% between the two fitting procedures; this provides an evaluation of the systematic error due to the combinatorial background subtraction. In fig.2, the resulting fit to the p–W opposite sign mass spectrum is shown with all the contributing processes. The Pb - Pb and S - U spectra have been fitted with the same procedure as adopted for the p - A data samples, without any constraint on the $\sigma_{D\overline{D}}/\sigma_{DY}$ ratio. The values of the combinatorial background R factor have been computed accordingly to the procedure outlined in section 4. The resulting fits satisfactorily describe the mass spectra for the 5 S - U and the 9 Pb - Pb centrality bins, but the open charm contribution increases, with respect to DY, with the size of the system and the centrality of the collision. We find a factor $\simeq 1.5$ enhancement from peripheral to central S - U and $\simeq 2$ from peripheral to central Pb - Pb collisions. Fig.3, shows the Pb–Pb fit for a peripheral and central bins.

6 Results

We can now compare our measured open charm yield with direct measurement of charmed hadron production. In a recent paper [19], results of various CERN and FNAL open charm hadro–production experiments have been re-

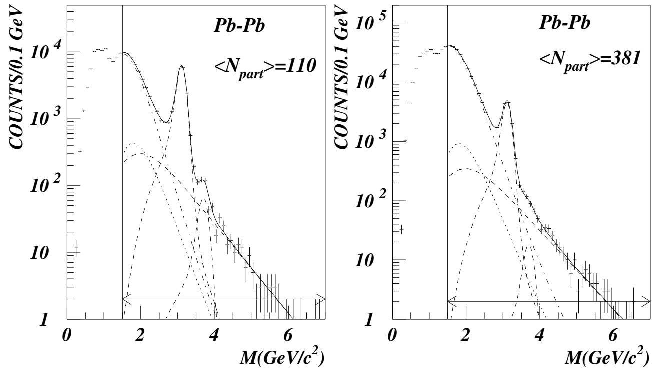

Figure 3: *Fit to peripheral and central Pb - Pb spectra. The DY, J/ψ and ψ' contributions are shown as dashed lines, the open charm as a dotted line, the background as a dashed–dotted line.*

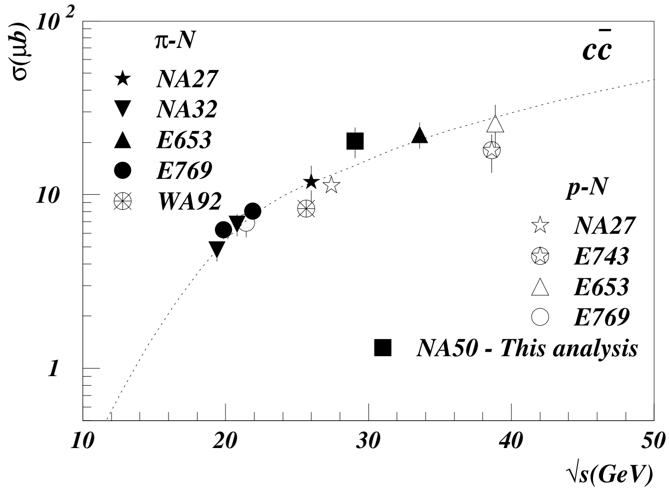

Figure 4: *Cross sections for forward (x_F>0) $c\bar{c}$ production compared with the value extrapolated from this analysis.*

viewed. The $\sqrt{s}$ dependence of D meson cross sections has been found to be well described by PYTHIA within a factor ~ 2, which can be attributed to residual systematic errors. The D meson differential distributions, as well as the lepton distributions from their semi–leptonic decays measured in several experiments, are in good agreement with PYTHIA calculations. To match the experimental points, the absolute normalization provided by PYTHIA must be scaled up by an appropriate K–factor.

Since PYTHIA reproduces the dilepton spectra from open charm and since the open charm and DY shapes have been here obtained with PYTHIA, we can extract the open charm cross-section from the open charm dimuon yield as measured from our fits. The resulting open charm cross section per nucleon for forward $c\bar{c}$ production as obtained from the p - A data sets is shown in fig.4, where it is compared with results from direct open charm measurements. The NA50 open charm cross section per nucleon extracted from the present analysis is in good agreement with the results from other experiments. The dotted line in fig.4 represents the PYTHIA prediction, scaled up by an ad-hoc K–factor. The S - U and Pb - Pb open charm cross sections per nucleon can be similarly computed and compared, at the relevant energies, with the points of fig.4. Either the dotted line in fig.4, or the same line re-scaled to match the NA50 p - A results, can be taken as a reference. In fig.5 the open charm enhancement with respect to the second reference, i.e. to the $c\bar{c}$ cross section normalized to the NA50 p - A point, is shown versus the number of participant nucleons N_{part} and for all the studied systems. The enhancement clearly increases with the collision centrality and the system size. In central Pb - Pb collisions the dimuon yield from open charm decays is 3 times higher than expected from a linear extrapolation of the observed p - A yield.

6.1 *The IMR dimuons p_T spectra*

To support the hypothesis of an open charm enhancement, we further check the p_T differential distributions where the DY and open charm contributions can be easily distinguished. The Monte–Carlo p_T spectra have been obtained in the same way as for the mass differential distributions. The DY, open charm and J/ψ contributions have been fixed using the results of the fits to the mass spectra, including the enhanced open charm. Fig.6 shows the p_T dimuon distributions, in the mass range $1.5 < M_{\mu\mu} < 2.5$ GeV/c^2, measured in peripheral and central Pb - Pb collisions. With no additional hypothesis, the superposition of the PYTHIA generated DY, open charm and J/ψ contributions, normalized accordingly to the results of the fit to the mass spectra, are in good agreement with the data.

7 Conclusions

The intermediate mass muon pair continua measured by the NA38/NA50 experiment in p - A, S - U and Pb - Pb collisions are well described as a superposition of dimuons from charmed meson (and baryon) semi-leptonic decays and DY, after combinatorial background subtraction. While in p - A collisions the open charm cross-section correctly scales with A, in S - U and Pb - Pb the dimuon production from open charm is enhanced with respect to the QCD expectations. The enhancement factor increases linearly with the number of participants and a factor 3 enhancement is found in central Pb - Pb colli-

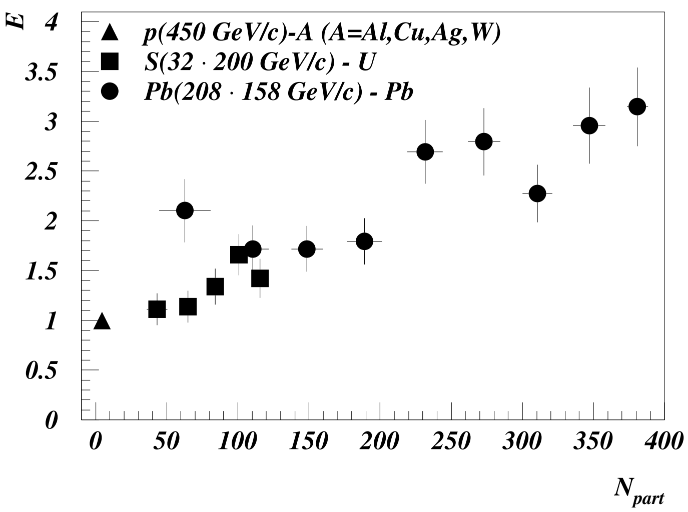

Figure 5: *The enhancement factor E of the open charm dimuon component with respect to p - A collisions versus the number of participant nucleons N_{part}.*

sions. The analysis of the intermediate mass region p_T spectra provides further support to the hypothesis that the excess dimuons originate from open charm decays.

References

1. For an overview on the subject see e.g., Ruuskanen P.V., *Nucl.Phys.*__A544__(1992)169c
2. Angelis A.L.S. *et al.* (HELIOS/3 Collaboration), preprint CERN-EP/98-92
3. Lourenço C. *et al.* (NA38 Collaboration), *Nucl.Phys.*__A566__(1994)77c
4. Scomparin E. *et al.* (NA50 Collaboration), *Nucl.Phys.*__A610__(1996)331c
5. Anderson L. *et al.*, *Nucl.Inst.Meth.* __223__(1984)26
6. S.Beolè, Pd.D. Thesis, Torino, Italy, 1998.
7. Arnaldi R. *et al.*, *Nucl.Inst.Meth.* __A411__(1998)1
8. Baglin C. *et al.* (NA38 Collaboration), *Phys.Lett.*__B220__(1989)471
9. Abreu M.C. *et al.* (NA50 Collaboration), *Phys.Lett.*__B410__(1997)327
10. Bellaiche F. *et al.*, *Nucl.Inst.Meth.* __A398__(1997) 180
11. Fleuret F., Thesis, Ecole Polytechinique, Palaiseau (1997)
12. Werner K., *Phys.Rep.* __232__(1993)87
13. Constantinescu S. *et al.*, preprint IPNO-DRE-96-01
14. Abreu M.C. *et al.* (NA50 Collaboration), *Phys.Lett.*__B410__(1997)337

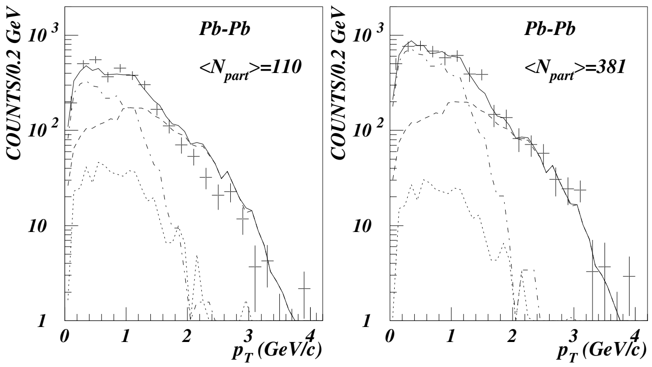

Figure 6: *The p_T distribution of IMR dimuons for peripheral and central Pb - Pb collisions. The DY (dashed line), J/ψ (dotted line) and $D\overline{D}$ (dashed-dotted line) individual contributions are shown separately, together with their sum (solid line).*

15. Leitch M.J. *et al.* (E789 Collaboration), *Phys.Rev.Lett.* __72__(1994)2542
16. Sjostrand T., *Computer Physics Commun.* __82__(1994)74
17. Martin A.D. *et al.*, *Phys.Rev.* __D51__(1995)4756
18. Alde D.M. *et al.* (E772 Collaboration), *Phys.Rev.Lett.*__64__(1990)2479
19. Braun-Munzinger P. *et al.*, *Eur.Phys.J.*__C1__ (1998)123